

Expanding universe with nonlinear gravitational waves

Taishi Ikeda^{*1}, Chul-Moon Yoo^{†1}, and Yasusada Nambu^{‡1}

¹*Departure of Physics, Graduate School of Science, Nagoya University, Nagoya 464-6602, Japan*

Abstract

We test the validity of Isaacson's formula which states that high frequency and low amplitude gravitational waves behave as a radiation fluid on average. For this purpose, we numerically construct a solution of the vacuum Einstein equations which contains nonlinear standing gravitational waves. The solution is constructed in a cubic box with periodic boundary conditions. The time evolution is solved in a gauge in which the trace of the extrinsic curvature K of the time slice becomes spatially uniform. Then, the Hubble expansion rate H is defined by $H = -K/3$ and compared with the effective scale factor L defined by the proper volume, area and length of the cubic box. We find that, even when the wave length of the gravitational waves is comparable to the Hubble scale, the deviation from Isaacson's formula $H \propto L^{-2}$ is at most 3% without taking a temporal average and is below 0.1% with a temporal average.

1 Introduction

The global aspect of our universe is well described by a homogeneous and isotropic FLRW (Friedmann-Lemaître-Robertson-Walker) metric. The homogeneity over the scale of 100Mpc is well established by many observations.

^{*}Electric address: ikeda@gravity.phys.nagoya-u.ac.jp

[†]Electric address: yoo@gravity.phys.nagoya-u.ac.jp

[‡]Electric address: nambu@gravity.phys.nagoya-u.ac.jp

At the same time, local inhomogeneity of our universe provides us a lot of information. One of the classical issue involved with the inhomogeneity is the so called backreaction problem(see e.g. [1–4]). Evaluation of the backreaction due to the local inhomogeneity on the global expansion law has been attracted much attention because large backreaction may cause significant systematic error for evaluation of the energy components of our universe.

One typical example of treating the backreaction is Isaacson’s formula [5, 6]. For gravitational waves with high frequency and low amplitude, Isaacson’s formula provides the coarse-grained effective energy momentum tensor which satisfies the traceless condition. Since the energy momentum tensor which is compatible with the homogeneity and isotropy is given by the perfect fluid form, Isaacson’s formula states that the high frequency and low amplitude gravitational waves behave like a radiation fluid on average (see Appendix B). Therefore, for a spatially flat FLRW universe with short wavelength gravitational waves, the relation between the Hubble parameter H and the scale factor a is expected to be $H \propto a^{-2}$.

The aim of this paper is to test the validity of Isaacson’s formula beyond the high frequency and low amplitude approximation. For the purpose, we consider the inhomogeneous universe which only contains the gravitational waves and calculate the time evolution of this universe. Because this universe is assumed to have no symmetry, it is inevitable to rely on a numerical computation to obtain its dynamics and we apply numerical relativity to tackle this problem. Over the past 20 years, numerical relativity has been extensively developed mainly for isolated systems. Recently, several authors applied the numerical relativity to the expanding or contracting universe models with aligned black holes and discussed the backreaction problem [7–10].

In this paper, we investigate the validity of Isaacson’s formula by solving the full Einstein equations with the use of numerical relativity. First, we construct the initial data which contains nonlinear gravitational waves by solving constraint equations of vacuum Einstein equations. This initial data is prepared in a cubic box with periodic boundary conditions between each pair of opposite faces of the box and corresponds to standing wave modes in the linear approximation. Concerning the time evolution, the backreaction effect of gravitational waves causes expansion or contraction of this universe. We use the gauge condition in which the trace of the extrinsic curvature K is spatially uniform. Then, the Hubble parameter is defined by $H = -K/3$. We introduce the effective scale factors L from the proper volume, proper area,

and proper length of this box. Isaacson's formula states that time evolution of this system is same as the universe with the radiation fluid in the short wavelength region and the Hubble parameter and the effective scale factors obey the relation

$$H = \frac{b}{L^2}, \quad (1)$$

where b is a constant. We evaluate the relation between the Hubble parameter H and the effective scale factor L in the numerically generated inhomogeneous universe and test the validity of this formula.

This paper is organized as follows. In Sec. 2, the initial data are constructed by solving constraint equations of the vacuum Einstein equations. We describe the time evolution of our model in Sec. 3 and the relation between the Hubble parameter H and the effective scale factor L is investigated. Furthermore, we report dependence of the initial amplitude on the dynamics in superhorizon scale and the effect of temporal average of the volume. Sec. 4 is devoted to a summary and discussion. We use units in which $c = G = 1$ throughout this paper.

2 Set up of initial data

2.1 Construction of initial data

As is mentioned in the introduction, we numerically construct a solution of the vacuum Einstein equations, which contains nonlinear standing gravitational waves in the cubic box with periodic boundary conditions. Naively thinking, since the gravitational waves have a positive energy, it causes the gravitational attractive force, so this system is unstable. Actually, as we will see later, this universe inevitably expands or contracts. In this section, we describe how to construct the initial data.

The initial data set is generated by solving the following Hamiltonian and momentum constraints:

$$\mathcal{R} + K^2 - K_{ij}K^{ij} = 0, \quad (2)$$

$$D_j K^j_i - D_i K = 0, \quad (3)$$

where \mathcal{R} is the scalar curvature of 3-metric γ_{ij} , K_{ij} is the extrinsic curvature, $K = \gamma^{ij}K_{ij}$, and D_i is the covariant derivative associated with γ_{ij} . For convenience, γ_{ij} and K_{ij} are decomposed into the conformal factor Ψ , conformal

3-metric $\tilde{\gamma}_{ij}$, and conformal traceless part of the extrinsic curvature \tilde{A}_{ij} as follows:

$$\begin{aligned}\gamma_{ij} &= \Psi^4 \tilde{\gamma}_{ij}, & \det(\tilde{\gamma}_{ij}) &= 1, \\ K_{ij} &= \Psi^4 \left(\tilde{A}_{ij} + \frac{1}{3} \tilde{\gamma}_{ij} K \right), & \tilde{\gamma}_{ij} \tilde{A}^{ij} &= 0.\end{aligned}\tag{4}$$

Using these variables, the Hamiltonian constraint and the momentum constraints are written as

$$\tilde{D}_i \tilde{D}^i \Psi - \frac{1}{8} \tilde{R} \Psi + \left(\frac{1}{8} \tilde{A}_{ij} \tilde{A}^{ij} - \frac{1}{12} K^2 \right) \Psi^5 = 0,\tag{5}$$

$$\tilde{D}_j \tilde{A}^{ij} + 6 \tilde{A}^{ij} \tilde{D}_j \ln \Psi - \frac{2}{3} \tilde{D}^i K = 0,\tag{6}$$

where \tilde{D}_i and \tilde{R} are the covariant derivative and the scalar curvature associated with $\tilde{\gamma}_{ij}$, respectively. In order to construct the initial data, we solve these constraints with appropriate ansatzes.

We assume that K is spatially constant and $\tilde{A}_{ij} = 0$. These assumptions make momentum constraints trivial. Furthermore, the Hamiltonian constraint is reduced to

$$\tilde{D}_i \tilde{D}^i \Psi - \frac{1}{8} \tilde{R} \Psi - \frac{1}{12} K^2 \Psi^5 = 0.\tag{7}$$

We also assume that the conformal metric has the following form:

$$\tilde{\gamma}_{ij} = \text{diag} \left(\frac{1 + h^{(3)}}{1 + h^{(2)}}, \frac{1 + h^{(1)}}{1 + h^{(3)}}, \frac{1 + h^{(2)}}{1 + h^{(1)}} \right),\tag{8}$$

where $h^{(i)} = \mathcal{A}^{(i)} \cos(\omega_0 x^{(i)} + \phi^{(i)})$, ($i = x, y, z$) [11]. A constant ω_0 specifies the coordinate wave number of the gravitational waves and $\phi^{(i)}$ is the phase of the gravitational waves. As we will see later, in the linear approximation, these ansatzes lead to a solution for standing gravitational waves with the amplitude $\mathcal{A}^{(i)}$. In this paper, for simplicity, we assume

$$\mathcal{A}^{(x)} = \mathcal{A}^{(y)} = \mathcal{A}^{(z)} = \mathcal{A}.\tag{9}$$

By this assumption, three spatial axes are equivalent to each other.

We consider periodic boundary conditions for each pair of opposite faces of the numerical box. The coordinate length of the edge of the box is set to

be $\lambda_0 = 2\pi/\omega_0$.¹ Under this boundary condition, without loss of generality, we can set

$$\phi^{(x)} = \phi^{(y)} = \phi^{(z)} = 0. \quad (10)$$

By integrating the Hamiltonian constraint over the box, we obtain

$$K = \pm \sqrt{-\frac{3 \int_{\text{box}} d^3x \sqrt{\tilde{\gamma}} \tilde{R} \Psi}{2 \int_{\text{box}} d^3x \sqrt{\tilde{\gamma}} \Psi^5}}, \quad (11)$$

where the first term in Eq. (7) has been reduced to the boundary integral and eliminated due to the periodic boundary conditions. Since the trace part of the extrinsic curvature gives the volume contraction rate, our solution describes expanding or contracting universe corresponding to negative or positive value of the extrinsic curvature, respectively.

Hamiltonian constraint (7) is invariant under the following scaling with a constant C :

$$\Psi \rightarrow C\Psi, \quad K \rightarrow K/C^2. \quad (12)$$

This ambiguity corresponds to a choice of the unit of the scale. In this paper, the normalization is fixed by

$$\int_{\text{box}} d^3x \sqrt{\gamma} \Psi = 1. \quad (13)$$

With the conditions (11) and (13), Eq. (7) is numerically integrated by using the successive over-relaxation (SOR) method.

We show that our initial data contains gravitational waves in the linear approximation $\mathcal{A} \ll 1$. It is worthwhile to note that, since $\tilde{R} = \mathcal{O}(\mathcal{A}^2)$, we obtain $K = \mathcal{O}(\mathcal{A})$ from Eq. (11) and $\Psi = 1 + \mathcal{O}(\mathcal{A}^2)$ from the Hamiltonian constraint (7). In this approximation, the conformal metric becomes

$$\tilde{\gamma}_{ij} \simeq \delta_{ij} + \text{diag}(h^{(3)} - h^{(2)}, h^{(1)} - h^{(3)}, h^{(2)} - h^{(1)}), \quad (14)$$

and the fluctuation part $\tilde{\gamma}_{ij} - \delta_{ij}$ satisfies the transverse traceless condition. Furthermore, for $\beta = 0$, as the equation of motion of $\tilde{\gamma}_{ij}$ is $\frac{\partial}{\partial t} \tilde{\gamma}_{ij} = -2\alpha \tilde{A}_{ij}$, $\tilde{A}_{ij} = 0$ means $\frac{\partial}{\partial t} \tilde{\gamma}_{ij} = 0$. Hence, the linearized form of our initial data $\tilde{\gamma}_{ij}$ corresponds to the standing gravitational waves at the moment of maximum amplitude.

¹In practice, 1/8 region of the box with reflection boundary condition is enough because of the discrete symmetry.

Remaning parameter \mathcal{A} corresponds to the initial amplitude of gravitational waves in the linear regime. In the short wavelength, the linear gravitational waves have only oscillatory modes and their amplitude decreases (increases) with expansion (contraction) of the universe. On the other hand, for the super horizon wavelength, the two modes of the gravitational waves correspond to the decaying mode and the growing mode. The ratio between these two modes is fixed by the phase of the gravitational waves at the horizon crossing. In our initial data, the phase of the gravitational standing waves is fixed so that the waves have the maximum amplitude at the initial time and the change of the value \mathcal{A} causes the change of the initial Hubble scale. Therefore the phase at the horizon crossing depends on \mathcal{A} and the behavior of the gravitational waves in the long wavelength regime also depends on the initial amplitude \mathcal{A} . We use initial data with $\mathcal{A} = 0.07, 0.08, 0.09, 0.1, 0.11$ and analyze the behavior of the metric both in the short wavelength region and long wavelength region.

3 Time evolution

To simulate the time evolution, we use the COSMOS code by appropriately modifying it for our purpose. The COSMOS code is an Einstein equation solver written in C++ by means of BSSN formalism [12, 13]. The algorithm of this code is similar to the SACRA code [14]. The COSMOS code has been used in papers [10, 15]. In the original code, the 4-th order finite differencing in space with uni-grid and the 4th order time integration with Runge-Kutta method in Cartesian coordinates are adopted. In this paper, we adopt the 2nd order central differencing in space and the leapfrog method with a time filtering for time integration. Because of the time reversal of the Einstein equation, the time evolution is simulated not only for the expanding universe with $K < 0$, but also for the contracting direction from the same initial data with $K > 0$. Our simulation has been terminated when the violation of the Hamiltonian constraint exceeds 1%.

3.1 Gauge condition

Before performing the time integration, we need to fix the gauge conditions for the lapse function α and the shift vector β^i . In regard to the shift vector, we set $\beta^i = 0$ for simplicity. As for the lapse function, we use the “uniform

K gauge” condition which keeps spatially uniform K on each time slice.

Let us derive the equation for the lapse function with the uniform K gauge. The time evolution equation of K is given by

$$\frac{\partial}{\partial t}K = -D_i D^i \alpha + \alpha \left(\tilde{A}_{ij} \tilde{A}^{ij} + \frac{K^2}{3} \right). \quad (15)$$

The uniform K gauge condition implies that the left hand side in this equation is spatially constant. Integrating this equation over the box, the time derivative of K is obtained by

$$\frac{\partial K}{\partial t} = \frac{\int_{\text{box}} d^3x \sqrt{\gamma} \alpha \left(\tilde{A}_{ij} \tilde{A}^{ij} + \frac{K^2}{3} \right)}{\int_{\text{box}} d^3x \sqrt{\gamma}}, \quad (16)$$

where the first term in the right hand side of Eq. (15) vanishes by virtue of Gauss’s theorem and the periodic boundary conditions. At every time step, we solve Eq. (15) by the SOR method to determined α .

3.2 Physical quantities

In order to test Isaacson’s formula (1), we investigate the relation between the effective Hubble parameter and the effective scale factor. Since our model is inhomogeneous, there is no unique definition of the Hubble parameter and the scale factor. Nevertheless, by virtue of the uniform K gauge condition, the Hubble parameter can be naturally defined as

$$H \equiv -\frac{K}{3}. \quad (17)$$

This definition coincides with the standard definition of H for the homogeneous and isotropic universe model.

One of the simplest definition of the scale factor is defined from the proper volume of the box:

$$L_V \equiv \left(\int_{\text{box}} dx dy dz \sqrt{\gamma} \right)^{1/3}. \quad (18)$$

We can also define other effective scale factors from the edge proper length and the surface proper area. These definitions are used in the several previous

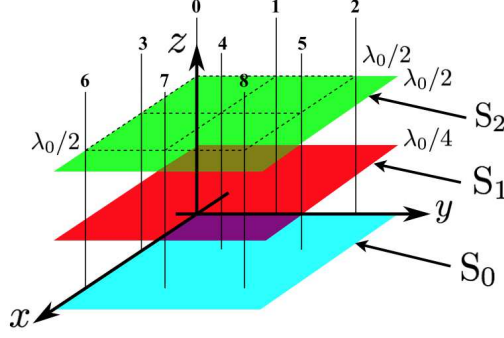


Figure 1: The box with periodic boundaries. The definitions of the lines 0-8 and surfaces $S_0(z = 0, \text{blue surface})$, $S_1(z = \lambda_0/4, \text{red surface})$ and $S_2(z = \lambda_0/2, \text{green surface})$ are shown.

works [7, 8, 10, 15–17]. The effective scale factors from the proper length and the proper area are

$$L_L(x, y) \equiv \int_0^{\lambda_0} dz \sqrt{\gamma_{zz}}, \quad (19)$$

$$L_A(z) \equiv \left(\int_0^{\lambda_0} dx dy \sqrt{\gamma_{xx}\gamma_{yy} - \gamma_{xy}^2} \right)^{1/2}. \quad (20)$$

Since L_L and L_A depend on x, y, z , we pick up the several characteristic positions as shown in Fig. 1. $L_A(z)$ is evaluated at $z = 0, \lambda_0/4, \lambda_0/2$ which are labeled as S_0, S_1 and S_2 , respectively. $L_L(x, y)$ is evaluated at $(x, y) = (0, 0), (0, \lambda_0/4), (0, \lambda_0/2), (\lambda_0/4, 0), (\lambda_0/4, \lambda_0/4), (\lambda_0/4, \lambda_0/2), (\lambda_0/2, 0), (\lambda_0/2, \lambda_0/4), (\lambda_0/2, \lambda_0/2)$, which are labeled as 0-8 lines, respectively.

In order to compare our numerical results with Isaacson's formula (1) in a precise sense, we must take not only spatial average but also temporal average. We consider the spatial average is taken by the definition of effective scale factors (18)-(20). However, for temporal average, we do not have any appropriate scale for the average, since our model has no exact periodicity along the time direction. One possible way for the temporal average is proposed and discussed in the Sec.4.3.

We evaluate the difference between the effective scale factor from our numerical result and that of Isaacson's formula as a function of the Hubble

parameter. The deviation is evaluated by

$$\delta_V(H) \equiv \frac{L_V - L_V^{\text{Isa}}}{L_V^{\text{Isa}}}, \quad (21)$$

$$\delta_A(H, z) \equiv \frac{L_A - L_A^{\text{Isa}}}{L_A^{\text{Isa}}}, \quad (22)$$

$$\delta_L(H, x, y) \equiv \frac{L_L - L_L^{\text{Isa}}}{L_L^{\text{Isa}}}, \quad (23)$$

where $L_V^{\text{Isa}}(H)$, $L_A^{\text{Isa}}(H, z)$ and $L_L^{\text{Isa}}(H, x, y)$ represent Isaacson's formula (1) and the coefficient b is determined by the least squares fitting of our numerical result in the region $L_V < \lambda_0$, which is attained by time evolution along the expanding temporal direction.

3.3 Convergence check

Let us consider the value of δ_V as a function of the grid spacing Δ . Since our numerical code has the second order accuracy, $\delta_V(\Delta)$ and its true value $\delta_{V\text{true}} \equiv \delta_V(0)$ are supposed to have the relation

$$\delta_V(\Delta) = \delta_{V\text{true}} + d\Delta^2 + \mathcal{O}(\Delta^3). \quad (24)$$

where a coefficient d is determined by numerical results. Using the two data sets taken with $\Delta = \Delta_1$ and Δ_2 , $\delta_{V\text{true}}$ and d can be obtained as

$$d = \frac{\delta_V(\Delta_1) - \delta_V(\Delta_2)}{\Delta_1^2 - \Delta_2^2} + \mathcal{O}(\Delta^3), \quad (25)$$

$$\delta_{V\text{true}} = \frac{\delta_V(\Delta_2)\Delta_1^2 - \delta_V(\Delta_1)\Delta_2^2}{\Delta_1^2 - \Delta_2^2} + \mathcal{O}(\Delta^3) \quad (26)$$

For $\Delta_1 = \lambda_0/120$ and $\Delta_2 = \lambda_0/100$, we calculate the value of d and $\delta_{V\text{true}}$. The value of convergence $(\delta_V(\Delta) - \delta_{V\text{true}})/d$ is compared with Δ^2 for each value of Δ in Fig. 2. We can clearly confirm that the second order convergence is achieved from Fig. 2. In the following, we use the numerical result with $\Delta = \lambda_0/120$.

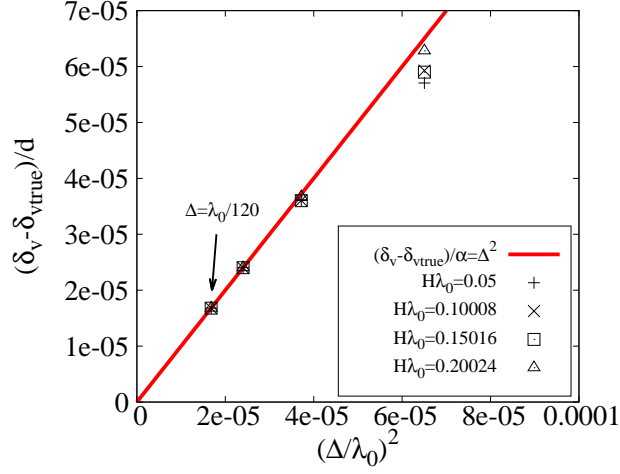


Figure 2: The convergence of $(\delta_V(\Delta) - \delta_{V\text{true}})/d$ at selected time steps. $\delta_{V\text{true}}$ and d are fixed by Eqs. (25) and (26).

4 Results of simulation

4.1 Relation between Hubble parameter and effective scale factor

In this subsection, we explain the relation between the Hubble parameter and the effective scale factors L_V , L_A , L_L for the initial amplitude $\mathcal{A} = 0.1$.

Before discussing the result, we introduce the characteristic Hubble parameter $H_{1.0}$, $H_{0.5}$ and $H_{0.1}$ by

$$L^{\text{Isa}}(H_{1.0}) = H^{-1}, \quad L^{\text{Isa}}(H_{0.5}) = 0.5H^{-1}, \quad L^{\text{Isa}}(H_{0.1}) = 0.1H^{-1}, \quad (27)$$

where $L^{\text{Isa}}(H) = \sqrt{b/H}$. That is, $H^{-1} = H_{1.0}^{-1}$ corresponds to the horizon crossing Hubble time. The parameter b in each $L^{\text{Isa}}(H)$ is determined by fitting the numerical data obtained by time evolution in expanding temporal direction. We define the short wavelength region $L^{\text{Isa}} < H^{-1}$ and the long wavelength region $L^{\text{Isa}} > H^{-1}$ in comparison with the Hubble scale.

The behavior of $L_V(H)$ and $\delta_V(H)$ is shown in Fig. 3.

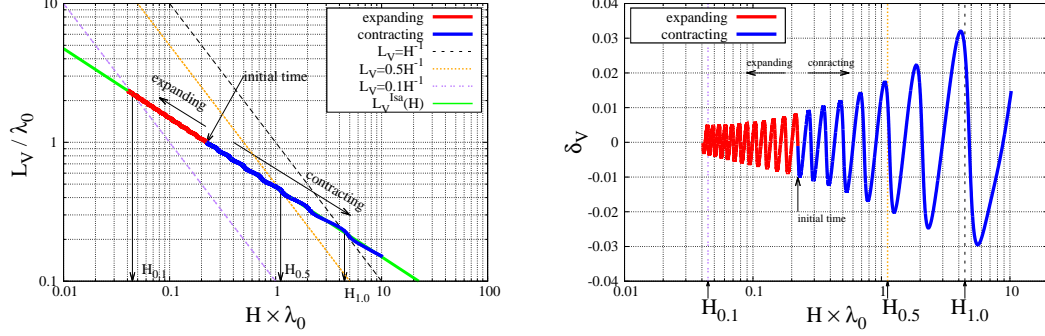


Figure 3: The behavior of $L_V(H)$. Isaacson's formula is $L_V^{\text{Isa}}(H) = \sqrt{b_V/H}$ with $b_V = 0.224$.

These figures show the oscillation of the scale factor which reflects the oscillation of gravitational waves. Our simulations have been terminated when the proper wave length L_V exceeds about $1.5/H$ in the contracting direction. It should be noted that Isaacson's formula is not guaranteed if the proper wave length becomes comparable to the Hubble scale. Nevertheless, Fig. 3 shows that the maximum value of the deviation from Isaacson's formula is about 3% and the deviation of central value from the formula is even smaller. Next, we show the behavior of $L_A(H)$ and $L_L(H)$. The behavior of $L_{A0}(H)$ (S_0 in Fig. 1), $L_{A1}(H)$ (S_1 in Fig. 1) and $L_{A2}(H)$ (S_2 in Fig. 1) are almost same as each other. Therefore, we plot only $L_{A0}(H)$.

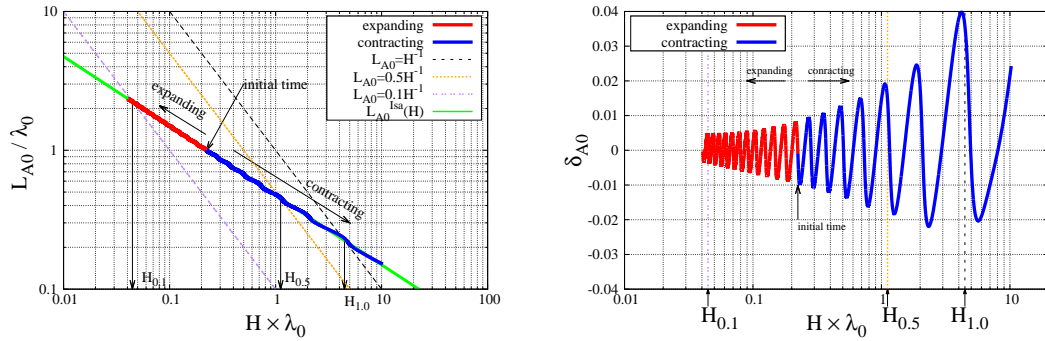


Figure 4: The behavior of $L_{A0}(H)$. Isaacson's formula is $L_{A0}^{\text{Isa}}(H) = \sqrt{b_{A0}/H}$ with $b_{A0} = 0.224$.

As is shown in Fig. 4, $L_{A0}(H)$ also oscillates in a similar way as $L_V(H)$. The maximum value of the deviation from Isaacson's formula around $H \sim H_{1,0}$ is about 4%, which is slightly larger than that of $L_V(H)$.

The relation $L_L(H)$ depends on the line position and can be classified into six types (Fig. 5). The behavior of $L_{L8}(H)$ and $\delta_{L8}(H)$ is similar to the behavior of $L_{L0}(H)$ and $\delta_{L0}(H)$. Furthermore, the behavior of $\delta_{L1}(H)$ and $\delta_{L3}(H)$ are almost same as $\delta_{L5}(H)$ and $\delta_{L7}(H)$ respectively, and the behaviors $\delta_{L2}(H)$ and $\delta_{L6}(H)$ have opposite phase to each other. Fig. 5 shows the value $\max(|\delta_{L0}| : H \sim H_{1,0}) = 15\%$ and $\max(|\delta_{L4}| : H \sim H_{1,0}) = 3\%$. On the other hand, $\max(|\delta_{L2}| : H \sim H_{1,0}) = 40\%$ and $\max(|\delta_{L6}| : H \sim H_{1,0}) = 60\%$, which are the maximum in any $\delta_L(H \sim H_{1,0})$.

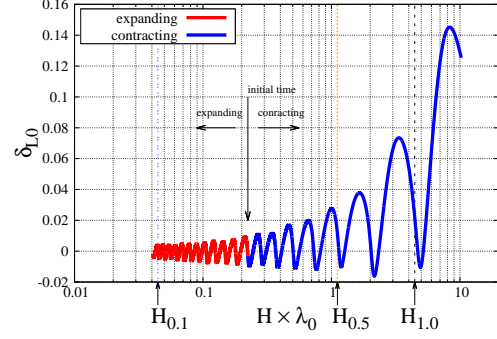
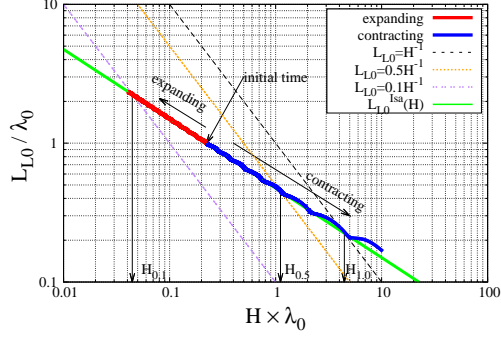
In order to understand these behaviors and make the position dependence of proper length clear, we consider our model with the linear approximation. As is mentioned in the Sec. 2, our model corresponds to the linear standing gravitational waves. Since all lines are parallel to z -axis, only γ_{zz} can contribute to the values of proper lengths among components of the conformal metric. For the standing gravitational waves, the time evolution of γ_{zz} is given by following form (see from appendix B)

$$\gamma_{zz} \simeq a(t)^2 \left\{ 1 + \frac{2\mathcal{A}}{a(t)} \cos \left(\int_0^t \frac{\omega_0 dt}{a(t)} + \phi \right) \cos \frac{\pi(x+y)}{\lambda_0} \cos \frac{\pi(x-y)}{\lambda_0} \right\}, \quad (28)$$

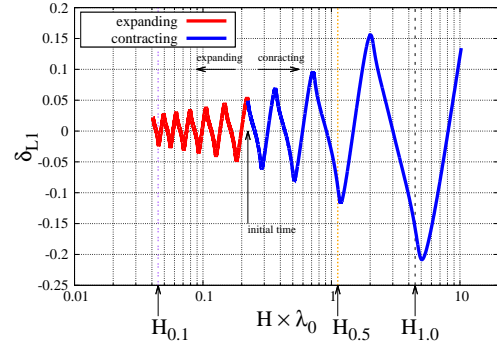
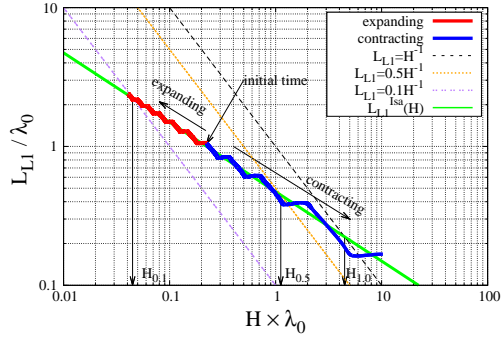
where ϕ is a constant determined by the condition $\frac{\partial}{\partial t} \tilde{\gamma}_{ij}|_{t=0} = 0$. According to Eq. (28), on the line 0, 4 and 8 with coordinates $(x, y) = (0, 0)$, $(\frac{\lambda_0}{4}, \frac{\lambda_0}{4})$, $(\frac{\lambda_0}{2}, \frac{\lambda_0}{2})$, γ_{zz} does not oscillate in the linear approximation. On the other hand, γ_{zz} on the line 2 and 6 with coordinates $(0, \frac{\lambda_0}{2})$, $(\frac{\lambda_0}{2}, 0)$ oscillate with amplitude $2\mathcal{A}$. Thus, in our model, the position dependence of the effective scale factor L comes from the difference of the amplitude of gravitational waves on each line, which is affected by the constructive interference of two oscillation modes $h^{(1)}$ and $h^{(2)}$ (see Eq. (14)). This result implies that, when we use a proper length as the effective scale factor, position dependence must be carefully treated.

4.2 The dependence of the initial amplitude \mathcal{A}

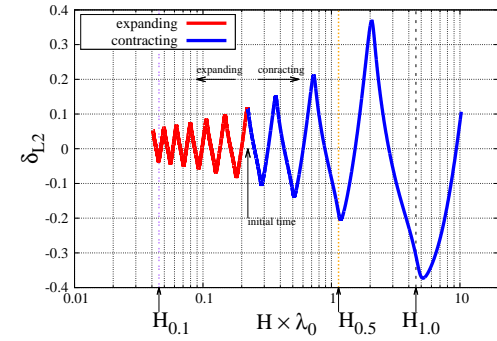
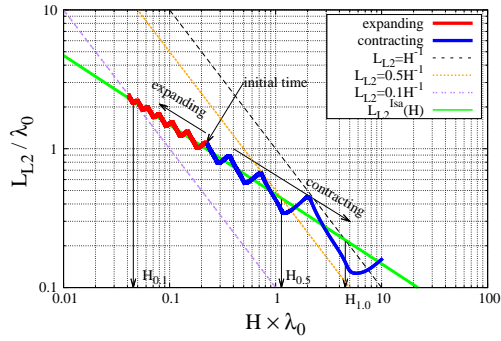
As is mentioned in the previous section, for the long wavelength ($L > 1/H$), gravitational waves are superposition of the decaying mode and the growing mode and their ratio depends on the phase of gravitational waves at the horizon crossing. Due to this phase dependence, the behavior of gravitational



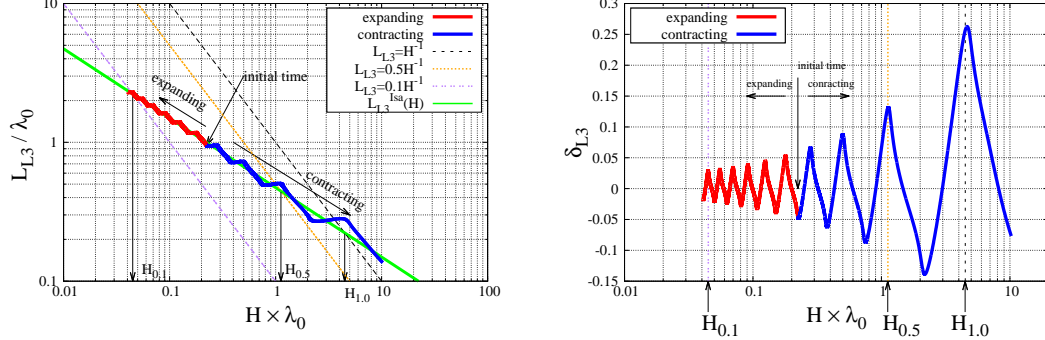
$L_{L0}(H)$: Isaacson's formula is $L_{L0}^{Isa}(H) = \sqrt{b_{L0}/H}$ with $b_{L0} = 0.224$.



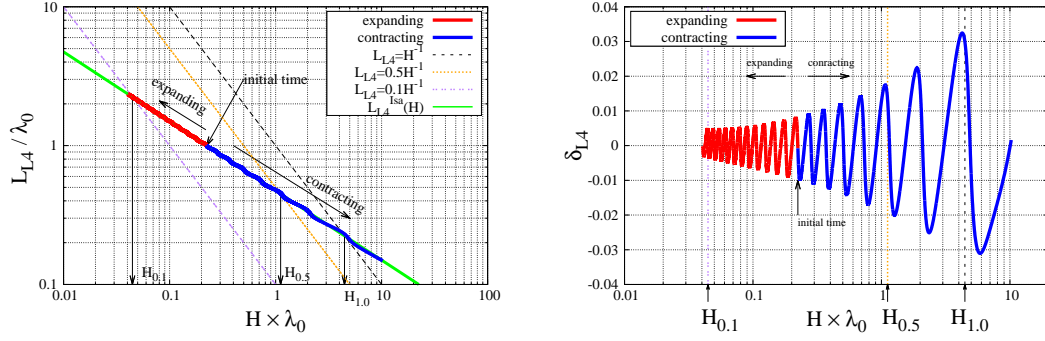
$L_{L1}(H)$: Isaacson's formula is $L_{L1}^{Isa}(H) = \sqrt{b_{L1}/H}$ with $b_{L1} = 0.223$.



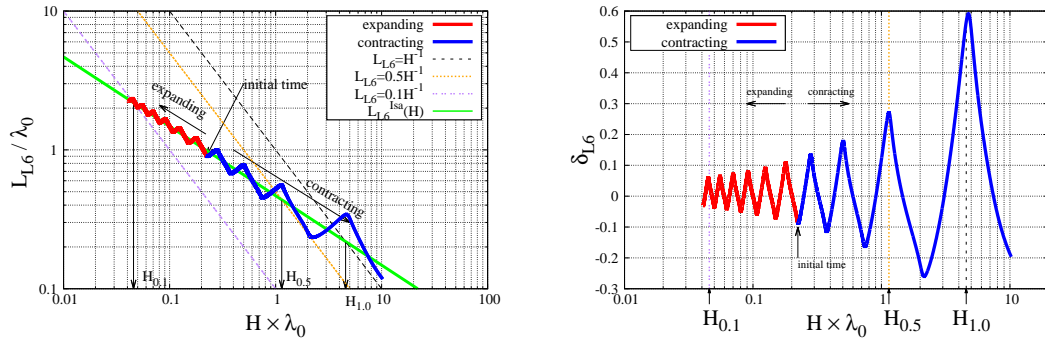
$L_{L2}(H)$: Isaacson's formula is $L_{L2}^{Isa}(H) = \sqrt{b_{L2}/H}$ with $b_{L2} = 0.220$.



$L_{L3}(H)$: Isaacson's formula is $L_{L3}^{\text{Isa}}(H) = \sqrt{b_{L3}/H}$ with $b_{L3} = 0.223$.



$L_{L4}(H)$: Isaacson's formula is $L_{L4}^{\text{Isa}}(H) = \sqrt{b_{L4}/H}$ with $b_{L4} = 0.224$.



$L_{L6}(H)$: Isaacson's formula is $L_{L6}^{\text{Isa}}(H) = \sqrt{b_{L6}/H}$ with $b_{L6} = 0.218$.

Figure 5: The characteristic behavior of $L_L(H)$ and $\delta_L(H)$.

waves depends on \mathcal{A} after the horizon crossing. In order to see this dependence, we focus on the time evolution of the Fourier component of γ_{xx} with the wave number $\vec{k} = (2\pi n_x/\lambda_0, 2\pi n_y/\lambda_0, 2\pi n_z/\lambda_0)$:

$$\gamma_{xx}(t, \vec{k}) \equiv \frac{1}{\lambda_0^3} \int_0^{\lambda_0} d^3x \gamma_{xx}(t, \vec{x}) \cos(\vec{k} \cdot \vec{x}). \quad (29)$$

For $\vec{k}_0 \equiv (0, 0, 2\pi/\lambda_0)$, the initial value of $\gamma_{xx}(t, \vec{k}_0)$ is given by

$$\gamma_{xx}(0, \vec{k}_0) = \frac{\mathcal{A}}{2} + \mathcal{O}(\mathcal{A}^2). \quad (30)$$

On the flat FLRW metric background, we can analytically calculate the behavior of linear gravitational waves. The metric can be expressed as follows:

$$ds^2 = -dt^2 + a(t)^2 \{\delta_{ij} + h_{ij}(t, \vec{x})\} dx^i dx^j, \quad (31)$$

where $a(t)$ is the scale factor of the background universe and $h_{ij}(t, \vec{x})$ is the transverse traceless tensor of gravitational waves in the linear approximation. The evolution equation for a Fourier mode $h_{ij}(t, \vec{k})$ of $h_{ij}(t, \vec{x})$ is given by (see Appendix B)

$$\frac{\partial^2}{\partial t^2} h_{ij}(t, \vec{k}) + 3H \frac{\partial}{\partial t} h_{ij}(t, \vec{k}) + \frac{1}{a^2} k^2 h_{ij}(t, \vec{k}) = 0. \quad (32)$$

Behavior of $h_{ij}(t, \vec{k}_0)$ for the short wavelength $k_0 > aH$ can be approximated by the WKB form as follows:

$$h_{ij}(t, \vec{k}_0) \simeq \frac{1}{a} h_{ij}|_{t=0} \cos\left(\int_0^t \frac{k_0 dt}{a}\right), \quad (33)$$

where we have used the normalization $a|_{t=0} = 1$. Let us assume that the time evolution of the background metric is given by that of radiation dominated universe,

$$a = \sqrt{2bt + 1}, \quad (34)$$

where $b = b_V$ and $a = L_V/\lambda_0$. From Eq. (33), the time evolution of the Fourier component is given by

$$a(t)^2 h_{xx}(t, \vec{k}_0) = a \frac{\mathcal{A}}{2} \cos\left[-\frac{1}{b\lambda_0} \left(\sqrt{2bt + 1} - \phi\right)\right], \quad (35)$$

where we have set $a^2 h_{xx}|_{t=0} = \gamma_{xx}|_{t=0}$ up to the leading order and ϕ is the integration constant.

We want to evaluate the deviation between $\gamma_{xx}(t, \vec{k}_0)$ and $a(t)^2 h_{xx}(t, \vec{k}_0)$. Since we have used the WKB and the linear approximation to derive the expression (35), when one of these approximations is violated, $a(t)^2 h_{xx}(t, \vec{k}_0)$ deviates from $\gamma_{xx}(t, \vec{k}_0)$. In our setting, this deviation may happen around the horizon crossing. After the horizon crossing even in linear regime, the “decaying mode” (for expanding universe) is enhanced and the deviation of our numerical solution from the linear WKB solution is expected. This deviation due to the decaying mode depends on the value of \mathcal{A} .

We introduce the deviation $\delta(t)$ as follows

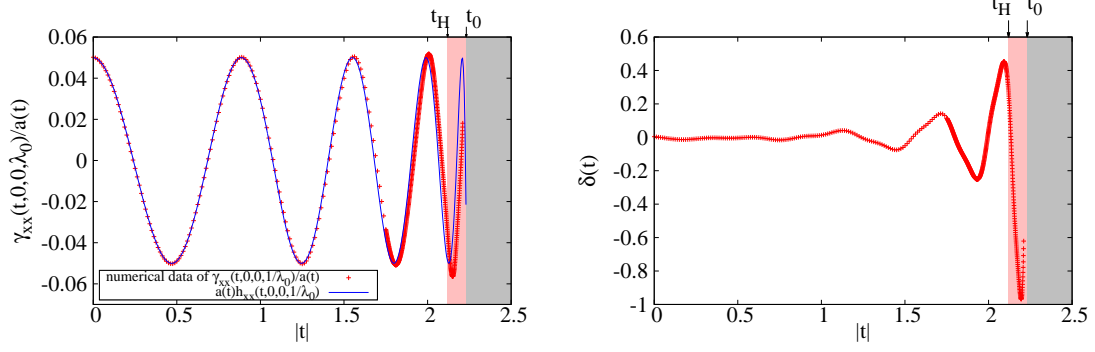
$$\delta(t) \equiv 2 \frac{\gamma_{xx}(t, \vec{k}_0) - a(t)^2 h_{xx}(t, \vec{k}_0)}{\mathcal{A} a(t)}. \quad (36)$$

The evolution of $\gamma_{xx}(t, \vec{k}_0)/a(t)$, $a(t)h_{xx}(t, \vec{k}_0)$ and $\delta(t)$ are shown in Fig. 6 for $\mathcal{A} = 0.1$, $\mathcal{A} = 0.11$ and $\mathcal{A} = 0.09$. Around the horizon crossing, the behavior of $\delta(t)$ depends on the value of \mathcal{A} . So, one may expect that the deviation from Isaacson’s formula depends on \mathcal{A} . Although the WKB approximation is violated around the horizon crossing, the values of δ_V and δ_A do not depend so much on the value of \mathcal{A} . On the other hand, we can see significant dependence of \mathcal{A} on δ_L . In particular, on the line 2 and 6, which correspond to anti-node of the standing waves, this dependence is large (for example, for $\mathcal{A} = 0.07, 0.08, 0.09, 0.1, 0.11$, $\max(|\delta_{L2}(H \sim 1/L_V)|)$ is 60%, 40%, 60%, 30%, and 40%, respectively).

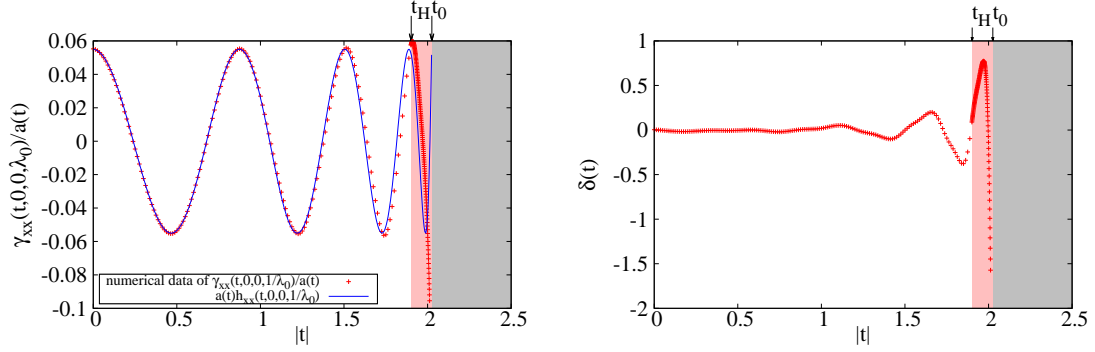
4.3 Temporal average

As is mentioned in Sec. 3.2, to compare our results with the original Isaacson’s formula, it is necessary to consider not only spatial average but also temporal one. The necessity of the temporal average is also explicitly shown in Appendix B for Isaacson’s formula in the FLRW universe. However, because of the lack of the temporal periodicity, the temporal averaging is fairly ambiguous in the present case. We consider the following temporal averaging:

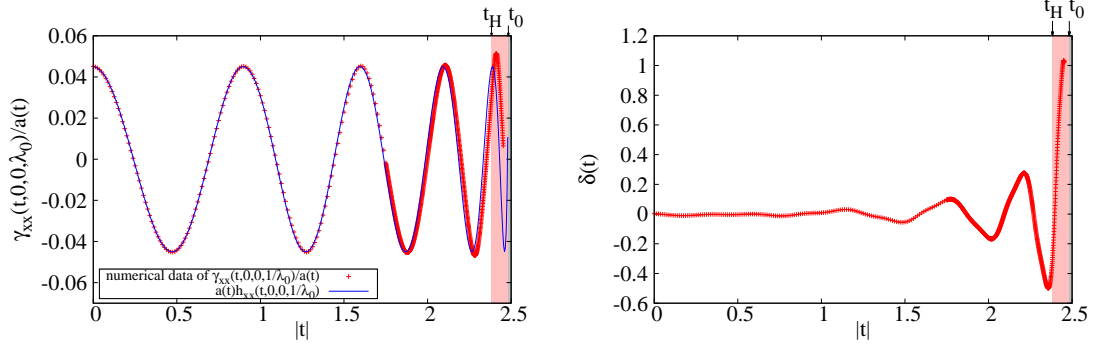
$$\langle L_V \rangle_{\text{tem}}(\eta) \equiv \frac{1}{\lambda_0} \int_{\eta-\lambda_0/2}^{\eta+\lambda_0/2} d\eta L_V, \quad (37)$$



$$\mathcal{A} = 0.1: \phi = 1.95.$$



$$\mathcal{A} = 0.11: \phi = 1.06.$$



$$\mathcal{A} = 0.09: \phi = 1.05.$$

Figure 6: Evolution of the Fourier component $\gamma_{xx}(t, \vec{k}_0)/a(t)$ (the left row) and the deviation (36) $\delta(t)$ (the right row). The integral constant ϕ in $h_{xx}(t, \vec{k}_0)$ is determined by fitting the numerical data in the region $0.0 < t < 1.0$. We define the horizon crossing time t_H and the big bang singularity time t_0 as $L_V^{\text{Isa}}(t_H) = H(t_H)^{-1}$ and $L_V^{\text{Isa}}(t_0) = 0$, respectively.

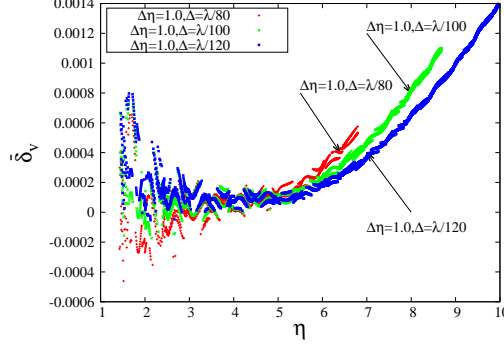


Figure 7: Evolution of $\bar{\delta}_V(\eta) = \frac{\langle L_V \rangle_{\text{tem}}(\eta) - L_V^{\text{Is}}(\eta)}{L_V^{\text{Is}}(\eta)}$ for different grid sizes. The red, green and blue lines are $\Delta = \lambda_0/80$, $\Delta = \lambda_0/100$ and $\Delta = \lambda_0/120$, respectively. The parameter b in the $L_V^{\text{Is}} = \sqrt{2bt+1}$ is 0.223, which is given by fitting the numerical data in the region $0.8 < L_V/\lambda_0 < 1$.

where $\eta = \int^t dt/a$ is the conformal time. We note that the comoving wavelength of the linear gravitational waves is λ_0 . For simplicity, we use the scale factor of the radiation dominated universe $a = \sqrt{2bt+1}$ ² as the scale factor in the definition of η , where b is given by fitting $\sqrt{2bt+1}$ to L_V/λ_0 in the region $L_V/\lambda_0 = [0.8, 1.0]$. Thus, the conformal time is rewritten as the following form: $\eta = a/b = 1/\sqrt{bH}$. The deviation $\bar{\delta}_V = \frac{\langle L_V \rangle_{\text{tem}}(\eta) - L_V^{\text{Is}}(\eta)}{L_V^{\text{Is}}(\eta)}$ is depicted as a function of η in Fig. 7. The value of $\bar{\delta}_V$ does not converge within our numerical precision because the $\bar{\delta}_V$ depends on Δ . Nevertheless, from this figure, it is suggested that the deviation $\bar{\delta}_V$ is at most $\sim 0.1\%$.

5 Summary and discussion

In this paper, we have investigated validity of Isaacson's formula by solving the Einstein equations with technique of numerical relativity. By solving the Hamiltonian constraint, we numerically constructed the initial data of the universe which contains the nonlinear standing gravitational waves in a cubic box with the periodic boundary. Then the time evolution was performed with the COSMOS code based on the BSSN formalism. In order to investigate the validity of Isaacson's formula, we calculated the relation

² In this discussion, we always consider expanding universe, thus the scale factor a is an increasing function of time.

between the effective scale factor and the Hubble parameter and compared it with Isaacson's formula. The effective scale factors are defined from the proper volume, proper area and proper length, and the Hubble parameter is defined from trace of the extrinsic curvature of the time slice. The results are summarized in Table 1. The deviation from Isaacson's formula δ_V is at

	$L \sim 1/H$	$L \sim 0.5/H$	$L \sim 0.1/H$
volume	$\delta_{V\max} \sim 3\%$	$\delta_{V\max} \sim 2\%$	$\delta_{V\max} \sim 0.5\%$
area	$\delta_{A\max} \sim 4\%$	$\delta_{A\max} \sim 2\%$	$\delta_{A\max} \sim 0.5\%$
length	$\delta_{L\max} \sim 60\%$	$\delta_{L\max} \sim 30\%$	$\delta_{L\max} \sim 5\%$

Table 1: The largest value of the deviations from Isaacson's formula are listed for each value of the effective scale factors L determined by the proper volume, area and length.

most about 3% in the range of our numerical calculation given by $L \lesssim 1/H$. Although Isaacson's formula is not guaranteed for $L \sim 1/H$, this formula has still a few % accuracy. Behavior of $L_{A0}(H)$, $L_{A1}(H)$ and $L_{A2}(H)$ are similar to that of the proper volume. While, for the effective scale factor defined by the proper length, deviation from the Isaacson's formula depends on the line position. This means that, when we use the proper length as the effective scale factor, the position dependence must be carefully treated. We also discussed the temporal average of the effective scale factor given by the proper volume, which gives a central value of the temporal oscillation of the effective scale factor. Our calculation of the temporal average suggests that the deviation of the central value from Isaacson's formula is at most $\sim 0.1\%$ in the range of our calculation.

One might expect that, when the gravitational wavelength is much longer than the Hubble scale, our model approaches to the Kasner solution. However, in our calculation, we could not proceed time evolution beyond $L \sim 1.5/H$. At this time, Hamiltonian constraint is violated, and we could not see any typical feature of the Kasner solution. Even using the finer resolution, the violation time does not change. This time t_c of the constraint violation is near the big bang singularity time $t_0 = \frac{1}{2\alpha}$ (see Eq. (34)):

$$|t_0 - t_c| \sim \frac{0.3}{H} \quad (\text{in the case of } \mathcal{A} = 0.1). \quad (38)$$

Therefore, this constraint violation would be originated from the big bang singularity. We need more refined numerical method to analyze the struc-

ture of the spacetime around the singularity [18]. Introducing another time coordinate, such as the e-folding number, we may investigate more details of the behavior in the early stage of the universe. We leave it as a future work.

Acknowledgements

We are grateful to Ken-ichi Nakao and Misao Sasaki for helpful discussions and comments.

Appendix

A Time evolution equations

Here, we summarize time evolution part of the Einstein equation in vacuum.

$$\left(\frac{\partial}{\partial t} - \mathcal{L}_\beta\right) \Psi = \frac{\Psi}{6} \left(\tilde{D}_i \beta^i - \alpha K\right), \quad (39)$$

$$\left(\frac{\partial}{\partial t} - \mathcal{L}_\beta\right) \tilde{\gamma}_{ij} = -2\alpha \tilde{A}_{ij} - \frac{2}{3} \tilde{D}_k \beta^k \tilde{\gamma}_{ij}, \quad (40)$$

$$\left(\frac{\partial}{\partial t} - \mathcal{L}_\beta\right) K = -\Psi^{-4} (\tilde{D}_i \tilde{D}^i \alpha + 2\tilde{D}_i \ln \Psi \tilde{D}^i \alpha) + \alpha [\tilde{A}_{ij} \tilde{A}^{ij} + \frac{K^2}{3}], \quad (41)$$

$$\begin{aligned} \left(\frac{\partial}{\partial t} - \mathcal{L}_\beta\right) \tilde{A}_{ij} = & -\frac{2}{3} \tilde{D}_k \beta^k \tilde{A}_{ij} + \alpha \left(K \tilde{A}_{ij} - 2\tilde{\gamma}^{kl} \tilde{A}_{ik} \tilde{A}_{jl} \right) \\ & + \Psi^{-4} \{ -\tilde{D}_i \tilde{D}_j \alpha + 2\tilde{D}_i \ln \Psi \tilde{D}_j \alpha + 2\tilde{D}_j \ln \Psi \tilde{D}_i \alpha \\ & + \frac{1}{3} (\tilde{D}_k \tilde{D}^k \alpha - 4\tilde{D}_k \ln \Psi \tilde{D}^k \alpha) \tilde{\gamma}_{ij} \\ & + \alpha [\tilde{R}_{ij} - \frac{1}{3} \tilde{R} \tilde{\gamma}_{ij} - 2\tilde{D}_i \tilde{D}_j \ln \Psi + 4\tilde{D}_i \ln \Psi \tilde{D}_j \ln \Psi \\ & + \frac{2}{3} (\tilde{D}_k \tilde{D}^k \ln \Psi - 2\tilde{D}_k \ln \Psi \tilde{D}^k \ln \Psi) \tilde{\gamma}_{ij}] \}, \end{aligned} \quad (42)$$

where α is the lapse function, β is the shift vector, \mathcal{L}_β is the Lie derivative with respect to β , and the other variable defined in Sec.2.

B Isaacson's formula in Friedmann universe

Isaacson investigated the effective energy momentum tensor of low amplitude and high frequency gravitational waves [5, 6] in general background. In this appendix, we derive the effective energy-momentum tensor of low amplitude and high frequency gravitational waves in the spatially flat FLRW universe. The full metric can be written as

$$ds^2 = -dt^2 + a^2(t) \{ \delta_{ij} + h_{ij}(t, \vec{x}) \} dx^i dx^j, \quad (43)$$

where $a(t)$ is the scale factor and h_{ij} is low amplitude and high frequency perturbation which satisfies the transverse and traceless gauge conditions: $\delta^{ij} h_{ij} = 0$, $\partial^i h_{ij} = 0$.

In order to consider the low amplitude and high frequency gravitational waves, we introduce a small parameter $\epsilon \ll 1$ and assume the following order of perturbation: $h_{ij} \sim \mathcal{A} \sim \lambda/l \sim \epsilon$, where \mathcal{A} is typical amplitude of gravitational waves λ is typical wavelength of gravitational waves, l is a typical scales of background Hubble scale in the present case. Then, we find $\partial_k h_{ij} \sim \epsilon^0$ and $\partial_l \partial_k h_{ij} \sim \epsilon^{-1}$.

We decompose the Ricci tensor by the order of ϵ as follows:

$$R_{\mu\nu} = \bar{R}_{\mu\nu}^{(0)} + R_{\mu\nu}^{(-1)} + R_{\mu\nu}^{(0)} + \mathcal{O}(\epsilon), \quad (44)$$

where we assign $\bar{R}_{\mu\nu}^{(0)} = \mathcal{O}(\epsilon^0)$ for the background part. Each terms are

$$\bar{R}_{00}^{(0)} = -\frac{3\ddot{a}}{a}, \quad (45)$$

$$\bar{R}_{0i}^{(0)} = 0, \quad (46)$$

$$\bar{R}_{ij}^{(0)} = (\ddot{a}a + 2\dot{a}^2)\delta_{ij}, \quad (47)$$

$$R_{00}^{(-1)} = 0, \quad (48)$$

$$R_{0i}^{(-1)} = 0, \quad (49)$$

$$R_{ij}^{(-1)} = \frac{a^2}{2} \left\{ \ddot{h}_{ij} - \frac{1}{a^2} \nabla^2 h_{ij} + 3H\dot{h}_{ij} \right\}, \quad (50)$$

$$R_{00}^{(0)} = \frac{1}{4a^2} \dot{h}_{ij} \dot{h}^{ij} + \frac{1}{2a^2} \ddot{h}_{ij} h^{ij}, \quad (51)$$

$$R_{0i}^{(0)} = \frac{1}{4a^2} \dot{h}_{kl} \partial_i h^{kl} + \frac{1}{2a^2} h_{kl} \partial_i \dot{h}^{kl} - \frac{1}{2a^2} h^{mn} \partial_m \dot{h}_{ni}, \quad (52)$$

$$R_{ij}^{(0)} = \frac{1}{4a^2} \partial_j h^{mn} \partial_i h_{mn} + \frac{1}{2a^2} h^{mn} \partial_i \partial_j h_{mn} + \frac{1}{2a^2} h^{mn} \partial_m \partial_n h_{ij}$$

$$\begin{aligned}
& - \frac{1}{2a^2} h^{mn} \partial_m \partial_j h_{ni} - \frac{1}{2a^2} h^{mn} \partial_m \partial_i h_{nj} - \frac{1}{2} \dot{h}_j^m \dot{h}_{mi} \\
& + \frac{1}{2a^2} \partial^n h_j^m \partial_n h_{mi} - \frac{1}{2a^2} \partial^n h_j^m \partial_m h_{ni},
\end{aligned} \tag{53}$$

and dot denotes the time derivative.

In our ordering of the perturbation, the leading order equation is given by

$$\frac{\partial^2}{\partial t^2} h_{ij}(t, \vec{x}) + 3H \frac{\partial}{\partial t} h_{ij}(t, \vec{x}) - \frac{1}{a^2} \nabla^2 h_{ij}(t, \vec{x}) = 0. \tag{54}$$

Using the WKB approximation, the solution is

$$h_{ij}(t, \vec{x}) = \frac{1}{a} \int \frac{l^3 d^3 k}{(2\pi)^3} (\mathcal{A}_{ij}^{(\vec{k})} u_{\vec{k}}(t) e^{i\vec{k} \cdot \vec{x}} + \text{c.c.}), \tag{55}$$

where $u_{\vec{k}}(t)$ is defined by

$$u_{\vec{k}}(t) = e^{i \int_0^t \frac{k}{a} dt}, \tag{56}$$

l is the size of the comoving box and $\mathcal{A}_{ij}^{(\vec{k})}$ is an integration constant which satisfies $\delta^{ij} \mathcal{A}_{ij}^{(\vec{k})} = 0$ and $k^i \mathcal{A}_{ij}^{(\vec{k})} = 0$.

In the next leading terms of the Einstein equations, we find the time evolution equation of the background. Since we are interested in the back-reaction effect of $h_{\mu\nu}$ on the dynamics of the background metric $\bar{g}_{\mu\nu}$, we extract homogeneous and isotropic part of contribution from $R_{\mu\nu}$. That is, we consider the following field equation

$$\bar{R}_{\mu\nu}^{(0)} - \frac{1}{2} \bar{R}^{(0)} \bar{g}_{\mu\nu} = 8\pi T_{\mu\nu}^{(\text{GW})}, \tag{57}$$

with the effective energy-momentum tensor is defined by

$$T_{\mu\nu}^{(\text{GW})} = -\frac{1}{8\pi} (\langle R_{\mu\nu}^{(0)} \rangle - \frac{1}{2} \bar{g}_{\mu\nu} \langle R^{(0)} \rangle), \tag{58}$$

where $\langle \rangle$ denotes a spatial average which smoothes out the inhomogeneities and extracts the spatially homogeneous and isotropic part. The average scale is assumed to be larger than the wavelength of gravitational waves and we explicitly describe how to take this average below.

First, to preserve the covariance of each variables under the spatial rotation, we impose the following property for the average for any physical quantity $Q(\vec{k}, \vec{k}')$:

$$\langle Q(\vec{k}, \vec{k}') u_{\vec{k}} u_{\vec{k}'}(t, x) \rangle = \langle Q(\vec{k}, \vec{k}') e^{i \int_0^t \frac{k+k'}{a} dt} e^{i(k_j+k'_j) \cdot x_j} \rangle$$

$$= \langle Q(\vec{k}, -\vec{k}) \rangle \frac{(2\pi)^3}{l^3} \delta(\vec{k} + \vec{k}') e^{i2 \int_0^t \frac{k}{a} dt}, \quad (59)$$

and

$$\begin{aligned} \langle Q(\vec{k}, \vec{k}') u_{\vec{k}}^* u_{\vec{k}'}(t, \vec{x}) \rangle &= \langle Q(\vec{k}, \vec{k}') e^{i \int_0^t \frac{-k+k'}{a} dt} e^{i(-k_j+k'_j) \cdot x_j} \rangle \\ &= \langle Q(\vec{k}, \vec{k}') \rangle \frac{(2\pi)^3}{l^3} \delta(\vec{k} - \vec{k}'). \end{aligned} \quad (60)$$

Substituting Eqs. (55) into Eq. (51) and (53), we obtain

$$\begin{aligned} \langle R_{00}^{(0)} \rangle &= - \int \frac{l^3 d^3 k}{(2\pi)^3} \left\{ \frac{3k^2}{4} \left(\mathcal{A}_{ij}^{(\vec{k})} \mathcal{A}_{ij}^{(-\vec{k})} e^{2i \int_0^t \frac{k}{a} dt} + \mathcal{A}_{ij}^{(\vec{k})*} \mathcal{A}_{ij}^{(-\vec{k})*} e^{-2i \int_0^t \frac{k}{a} dt} \right) \right. \\ &\quad \left. + \frac{k^2}{2a^4} \left| \mathcal{A}_{ij}^{(-\vec{k})} \right|^2 \right\}, \end{aligned} \quad (61)$$

$$\begin{aligned} \langle R_{ij}^{(0)} \rangle &= - \left\langle \int \frac{l^3 d^3 k}{(2\pi)^3} \left\{ \frac{k_i k_j}{4a^2} \left(\mathcal{A}_{kl}^{(\vec{k})} \mathcal{A}_{kl}^{(-\vec{k})} e^{2i \int_0^t \frac{k}{a} dt} + \mathcal{A}_{kl}^{(\vec{k})*} \mathcal{A}_{kl}^{(-\vec{k})*} e^{-2i \int_0^t \frac{k}{a} dt} \right) \right. \right. \\ &\quad - \frac{k^2}{a^2} \left(\mathcal{A}_{ik}^{(\vec{k})} \mathcal{A}_{jk}^{(-\vec{k})} e^{2i \int_0^t \frac{k}{a} dt} + \mathcal{A}_{ik}^{(\vec{k})*} \mathcal{A}_{jk}^{(-\vec{k})*} e^{-2i \int_0^t \frac{k}{a} dt} \right) \\ &\quad \left. \left. - \frac{3k_i k_j}{2a^2} \left| \mathcal{A}_{kl}^{(\vec{k})} \right|^2 + \frac{k^2}{a^2} \left(\mathcal{A}_{ik}^{(\vec{k})} \mathcal{A}_{jk}^{(\vec{k})*} + \mathcal{A}_{ik}^{(\vec{k})*} \mathcal{A}_{jk}^{(\vec{k})} \right) \right\} \right\rangle. \end{aligned} \quad (62)$$

The Ricci scalar $R^{(0)}$ is given by

$$\langle R^{(0)} \rangle = \frac{3}{2a^4} \int \frac{l^3 d^3 k}{(2\pi)^3} k^2 \left(\mathcal{A}_{ij}^{(\vec{k})} \mathcal{A}_{ij}^{(-\vec{k})} e^{2i \int_0^t \frac{k}{a} dt} + \mathcal{A}_{ij}^{(\vec{k})*} \mathcal{A}_{ij}^{(-\vec{k})*} e^{-2i \int_0^t \frac{k}{a} dt} \right). \quad (63)$$

Then, $T_{00}^{(\text{GW})}$ is given by

$$T_{00}^{(\text{GW})} = \frac{1}{2a^4} \int \frac{l^3 d^3 k}{(2\pi)^3} k^2 \left| \mathcal{A}_{ij}^{(\vec{k})} \right|^2. \quad (64)$$

By extracting the trace part, we obtain

$$\begin{aligned} T_{ij}^{(\text{GW})} &= \frac{\delta_{ij}}{2a^2} \int \frac{l^3 d^3 k}{(2\pi)^3} k^2 \left\{ \left(\mathcal{A}_{kl}^{(\vec{k})} \mathcal{A}_{kl}^{(-\vec{k})} e^{2i \int_0^t \frac{k}{a} dt} + \mathcal{A}_{kl}^{(\vec{k})*} \mathcal{A}_{kl}^{(-\vec{k})*} e^{-2i \int_0^t \frac{k}{a} dt} \right) \right. \\ &\quad \left. + \frac{1}{3} \left| \mathcal{A}_{kl}^{(\vec{k})} \right|^2 \right\}. \end{aligned} \quad (65)$$

The first and the second terms inside the integration of Eq. (65) are temporally oscillating, and we may eliminate this term by taking a temporal average and get following form:

$$T_{ij}^{(\text{GW})} = \frac{\delta_{ij}}{6a^2} \int \frac{l^3 d^3 k}{(2\pi)^3} k^2 \left| \mathcal{A}_{kl}^{(\vec{k})} \right|^2. \quad (66)$$

According to (64) and (66) , we obtain traceless energy momentum tensor like the radiation fluid. It means that the energy density of the effective energy momentum tensor is proportional to $1/a^4$.

References

- [1] G. F. R. Ellis, *Class. Quantum Grav.* **28**, 164001 (2011)
- [2] S. R. Green and R. M. Wald, *Class. Quantum Grav.* **31**, 234003 (2014)
- [3] Y. Nambu, *Phys. Rev. D* **62** (2000) 104010
- [4] T. Kai, H. Kozaki, K. i. Nakao, Y. Nambu and C. M. Yoo, *Prog. Theor. Phys.* **117**, 229 (2007)
- [5] R. A. Isaacson, *Phys. Rev.* **166**, 1263 (1967).
- [6] R. A. Isaacson, *Phys. Rev.* **166**, 1272 (1968).
- [7] E. Bentivegna and M. Korzynski, *Class. Quantum Grav.* **29**, 165007 (2012)
- [8] C. M. Yoo, H. Abe, K. i. Nakao and Y. Takamori, *Phys. Rev. D* **86**, 044027 (2012)
- [9] E. Bentivegna and M. Korzynski, *Class. Quantum Grav.* **30**, 235008 (2013)
- [10] C. M. Yoo and H. Okawa, *Phys. Rev. D* **89**, no. 12, 123502 (2014)
- [11] K. i. Nakao private communication,
- [12] M. Shibata and T. Nakamura, *Phys. Rev. D* **52**, 5428 (1995).
- [13] T. W. Baumgarte and S. L. Shapiro, *Phys. Rev. D* **59**, 024007 (1999)
- [14] T. Yamamoto, M. Shibata and K. Taniguchi, *Phys. Rev. D* **78**, 064054 (2008)
- [15] C. M. Yoo, H. Okawa and K. i. Nakao, *Phys. Rev. Lett.* **111**, 161102 (2013)

- [16] T. Clifton and P. G. Ferreira, *Phys. Rev. D* **80**, 103503 (2009) [*Erratum-
ibid. D* **84**, 109902 (2011)]
- [17] T. Clifton, K. Rosquist and R. Tavakol, *Phys. Rev. D* **86**, 043506 (2012)
- [18] D. Garfinkle, *Phys. Rev. Lett.* **93**, 161101 (2004)